Biomechanics of Pressure Ulcer in Body Tissues Interacting with External Forces during Locomotion

Arthur FT Mak, Ming ZHANG, Eric WC TAM

Department of Health Technology and Informatics

The Hong Kong Polytechnic University

15 October 2009

Correspondence Address:

Arthur FT Mak, PhD

Chair Professor of Rehabilitation Engineering

The Hong Kong Polytechnic University

Hunghom, Kowloon

Hong Kong

Tel: 852-3400-2601

Fax: 852-2334-1997

Email: arthur.mak@inet.polyu.edu.hk

ABSTRACT

Forces acting on the body via various external surfaces during locomotion are needed to support the body under gravity, control posture, and overcome inertia. Examples include the forces acting on the body via the seating surfaces during wheelchair propulsion, the forces acting on the plantar foot tissues via the insole during gait, and the forces acting on the residual limb tissues via the prosthetic socket during various movement activities. Excessive exposure to unwarranted stresses at the body support interfaces could lead to tissue breakdowns commonly known as pressure ulcers, presented often as deep tissue injuries around bony prominences and/or surface damages on the skin. In this paper, we review the literatures on how the involved tissues respond to epidermal loadings, taking into account both experimental and computational findings from in-vivo and in-vitro studies. In particular, related literatures on internal tissue deformation and stresses, microcirculatory responses, as well as histological, cellular and molecular observations are discussed.

Key Words: Tissue Biomechanics, Skin, Pressure Ulcer, Deep Tissue Injury, Ischemic Reperfusion, Rehabilitation Engineering

CONTENT

1. INTRODUCTION

Pressure ulcer is local tissue damage due to prolonged excessive loading acting on the skin via a body support surface. There are broadly speaking two forms of pressure ulcer - superficial and deep ulcers. Both are induced by prolonged excessive epidermal loadings. Superficial ulcers primarily involve frictional abrasive rubbing of the skin relative to the supporting surface and engage mostly the superficial tissues. Tissue damages could also start deep near the bony interface of skeletal prominences under epidermal loadings (1). Such deep ulcers if unattended could in time become massive lesions all the way to the skin.

About 85% of subjects with spinal cord injury (SCI) will develop a pressure ulcer during their lifetime (2, 3). Ischial tuberosity is the most common site for pressure ulcer (3). About 20% of the hospitalization of diabetic patients are due to foot problems (4). In industrialized countries, diabetes mellitus with insensitive feet is the main reason for foot pressure ulcers that could ultimately lead to lower limb amputations (5, 6). Amputees wearing prosthesis need to accommodate high ambulatory loadings during their daily activities. Those loadings are mostly transmitted from the prosthesis to the skeletal structure via the interface between a prosthetic socket and the soft tissues around the residual limb. The involved soft tissues are not used to those high epidermal pressure and shear loadings during locomotion. It is not uncommon for amputees to develop skin problems on the residual limb, such as blisters, cysts, edema, dermatitis, etc. (7, 8, 9).

Pressure ulcer can be viewed primarily as a biomechanical issue, although the cascade of clinical events often involve many confounding intrinsic and extrinsic factors, such as the general health condition and the personal hygiene of the subject involved. Decades

of research have clarified some mechanisms leading to pressure ulcers, though considerable controversies still remain. The methods for clinical prevention / intervention for pressure ulcer have had little breakthroughs, despite the enormous magnitude of the clinical problem and the recent advances in medical science and practice (10).

2. THE INVOLVED TISSUES

The tissues involved are highly complex. Their exact morphology and composition vary from site to site. It is essential to appreciate the details of the anatomical features of the particular sites experiencing ulcer, such as the tissues at the ischial tuberosities, the plantar foot tissues at the metatarsals, the deformation-sensitive tissues around a residual limb, etc.

Epidermis is made up of keratinizing stratified epithelium with a horny layer of flattened hexagonal anucleate cells forming a protective barrier at the top, and at the bottom a proliferative basal layer of stems cells for maintaining the epidermal layer. Most epidermal cells are keratinocytes with cytoskeletal filaments rich in keratin polypeptides, giving the cells and epidermis their biomechanical properties (11).

Dermis is a layer of connective tissues with blood vessels, lymphatics, sensory receptors, nerves, sweat glands and hair follicles. There are two sub-layers within the dermis – the papillary layer with a relatively loose collagen-elastin extracellular matrix and the reticular layer with coarser bundles running more parallel to the epidermis. These bundles become more randomly oriented further down (12). Most of the dermal collagens are of type I and type III, and are responsible for skin's tensile stiffness and strength, whereas elastins are known to be responsible for skin's elasticity. The collagen-elastin fibrous network entangles with and encapsulates a macromolecular gel of proteogylcans, made up primarily of hydrophilic poly-anionic dermatan sulfates, chondrotin sulfates, and hyaluronic acid. The proteoglycan gel is important in maintaining the spatial structure of the collagen-elastin network and in supporting skin's

capacity to carry compressive loading. Most dermal cells are fibroblasts. They are responsible to synthesize and thus upkeep the tissue's extracellular matrix.

The subcutaneous layer consists of adipose tissues of variable thickness depending on site. Deeper below are the deep fascia and muscles. Those deep tissues covering the bony prominences like the ischial tuberosities and the metatarsal heads are potential sites of deep tissue injuries under prolonged excessive epidermal loading.

In skin, blood enters through perforating arteries originating from the underlying vessels in the muscles, forming two major horizontal vascular networks – the deep dermal vascular plexus lying near the dermal–hypodermal interface, and the superficial subpapillary vascular plexus lying at the papillary–reticular interface in the dermis. The two vascular plexuses are linked by vertical vessels through the dermis. From the subpapillary plexus, some capillaries loop into the dermal papillae, extending close to the epidermis before returning back to the venous plexus located underneath the arteriolar papillary plexus. The deep dermal plexus emanates vessels deep into the adipose tissues and supplies blood to the sweat glands and hair follicles (11).

Microcirculation is driven by the spontaneous rhythmic vasomotion facilitated by the surrounding muscle cells. Vasomotion plays an important role in regulating blood flow in terminal arterioles and capillaries further downstream in the circulatory network. The lymphatic vessels collect excess interstitial fluid and protein that escape from capillaries and return them to the venous system.

Skin is innervated with mechanoreceptors for touch, pressure and pain sensing, such as the tactile corpuscles in the dermal papillae, and the Vater-Pacini corpuscles at the

dermal-hypodermal interface. Some of the skin sensory neurons are myelinated. Nociceptors are sensory neurons that can initiate painful sensations, including those induced mechanically. Their sensitivity can be affected by injuries or inflammation (13).

3. THE BIOMECHANICAL PROPERTIES OF THE INVOLVED TISSUES

The biomechanical properties of skin and the underlying tissues are anisotropic, inhomogeneous, and nonlinearly viscoelastic. These properties can change with ageing and pathological conditions (14, 15). Measurements of the in-vivo properties of skin and the subcutaneous tissues have been reported. (16-32).

3.1 Buttock Tissues

Human buttock consists of the pelvic bone, gluteal muscles and an adipose tissue layer under the cutaneous cover. The material properties and thicknesses of these buttock tissues play important roles in load transfer during seated mobility. Using ultrasound, the thickness of the soft tissues overlying the ischial tuberosity was measured to be 26.6 mm in healthy subjects and 24.1 mm in SCI subjects (33). The findings were similar to those measured using computer tomography (CT) (34). The average gluteal subcutaneous fat thickness was estimated to be 28.1mm. Based on magnetic resonance imaging (MRI), it was found that tissues overlying the ischial tuberosity during sitting were about 33.5mm thick in healthy subjects and 23.5mm thick among the SCI (35).

Using indentation and assuming a Poisson's ratio of 0.49, a Young's modulus of 15.2 kPa was reported for human buttock tissues (36). Using the inverse finite element method together with an iterative optimization process, the long-term shear modulus for skin/fat was about 1.2 kPa as compared to 1.0 kPa for muscle (32). Significant stiffening of the rat gracilis muscle concomitant with muscle cells death was demonstrated after the muscle was subjected to 35kPa compression for 30 minutes (37).

3.2 Plantar Foot Tissues

In vivo mechanical properties of plantar foot soft tissues have been measured mainly using indentation tests. Tissue deformation was monitored either by linear variable differential transformers (LVDT) or by ultrasound. Measurements at different plantar foot regions showed a range of Young's modulus from 43kPa to 120kPa (28). The exact values depend on the site, subject group, loading speed, and range of deformation. The Young's modulus of the heel tissues is highly nonlinear, with an initial Young's modulus of 105kPa and reaching 306kPa at 30% strain (30). A non-linear hyperelastic model has been used to describe these soft tissues properties (31, 38, 39).

The properties of the plantar foot tissues were posture dependent, possibly due to muscle contraction. The tissues became stiffer with dorsi-flexion and plantar-flexion, as compared with measurements made with the ankle in neutral position (28). The plantar soft tissues for diabetic subjects were found stiffer and thinner than normal, especially around the first metatarsal head (28, 30, 40). Such differences were not observed in (31).

3.3 Residual Limb Tissues

In vivo indentation tests have been used to measure the mechanical properties of residual limb soft tissues in both transtibial and transfemoral amputees (29). The Young's modulus of the residual limb tissues were reported to be around 60kPa (41), 50 to 145kPa (42), and10.4-89.2kPa (26).

Using ultrasonic Doppler system, it was found that the superficial tissue had significantly higher modulus than the tissue beneath (20). The moduli was found to be 145kPa,

50kPa, 50kPa and 120kPa for patellar tendon, popliteal, anteromedial and anterolateral sites respectively (42). Approximately 45% increase in stiffness was observed with muscle contraction (22). The nonlinear elasticity was also described using James-Green-Simpson material formulation and the material coefficients were found to depend on subject, site and loading speed (43).

4. THE INVOLVED EXTERNAL FORCES - STRESSES AT THE BODY SUPPORT INTERFACES

Interface stresses between the body and its support surfaces depend on the anatomical sites and are consequence of gravity, the geometry of the body tissues and their biomechanical properties, the contour and the stiffness of the external support surface, the friction at the interface, the body's orientation and its dynamic activities.

4.1 Stresses at the Buttock / Seating Interface

Many systems have been developed utilizing electro-pneumatic, resistive and capacitive transducers to assess interface pressure. The accuracy, creep and hysteresis of the readings of these measurements have been reported (44-46). Interface pressure was found altered after a pressure mat was introduced between a physical buttock phantom and seven test cushions, indicating that there was significant interaction between the cushions and pressure mat (47). It was reported that interface pressure under the ischial tuberosities when sitting on 3 inches of standard foam ranged from 8 to 19.5kPa.

Reported data on interface shear at the buttock/seat interface are sporadic. According to (48), the mean shear stresses underneath the tuberosities on three different types of cushions (low shear, gel and foam) were 4.8kPa, 6.4kPa and 6.7kPa respectively. It should be noted that these findings were highly dependent on the mechanical characteristics of the cushion material, buttock tissues and the sensor itself.

Taking into consideration of the influence of pressure mat on interface stress measurement, parameters such as peak pressure index, pressure gradient, pressure

distribution symmetry and contact area were used to interpret the buttock/seating interface condition for clinical assessment (49). Multistage longitudinal analysis and self-registration technique were introduced to examine the changes of interface pressure between pre- and post interventions (50). After carefully aligning the pressure images acquired, this technique utilized a statistical algorithm to analyse each pixel on the pressure mat at different time intervals to detect significant pressure changes. This technique can be applied to study the changes of dynamic pressure at the buttock/seat interface during activities and wheeled mobility.

Various researchers (51-53) have examined the dynamic interface pressure during wheelchair activities. In (53), the dynamic seating pressure during wheelchair propulsion was studied using a pressure mat on a rigid seat surface. Body kinematics was monitored using a motion analysis system. The spatial orientation of the pelvis was defined by the locations of the left and right anterior superior iliac spines (ASIS) and the two posterior superior iliac spines (PSIS) with the use of reflective markers. The spatial locations of the ischial tuberosities (IT) were derived assuming the pelvis as a rigid body. Pelvic tilting during wheelchair propulsion was found to be about 11.2 degrees for the normal group and 5.2 degrees for SCI. It was found that the dynamic positions of the ischial tuberosities as predicted from the motion analysis data did not exactly concur with the dynamic peak pressure locations as measured on the pressure mat. The dynamic peak pressure locations were located at about 19.2 mm anterior to the predicted locations of the ischial tuberosities. (Figure 1) Such anterior shift of the peak pressure location was bigger than the estimated predication error of the assumed model. The anterior shift of the peak pressure location was regarded reasonable given the associated pelvic rocking motion. One could also predict that when the hand was pushing the rim forward during forward propulsion, there would likely be a forward shear

traction acting on the buttock surface by the seat, assuming negligible reactions from the footrest and the backrest. Such forward shear traction could further accentuate the compaction of the tissues anterior to the contact zone.

4.2 Stresses at the Plantar Foot / Insole Interface

The stress distribution at the plantar foot / insole interface can reveal the biomechanical function of the foot and the effects of the shapes and materials of the foot supports in locomotion. The in-shoe pressure measurement techniques were reviewed in (54-56).

The structural and functional predictors of regional peak pressures under the foot in normal subjects during walking were evaluated in (57). Factors examined in this study included anthropometric data, passive range of motion, measurements taken from weight-bearing radiographs, properties of the plantar foot tissues, kinematics, electromyographs, etc. It was shown that heel pressure depended on longitudinal arch structure, heel pad thickness, linear kinematics and age; and pressure under the first metatarsal head depended on radiographic measures, talocrural dynamic range of motion, and gastrocnemius EMG activity.

The peak plantar pressure and peak pressure gradient at the forefoot/insole interface during walking were compared among normal subjects, diabetic subjects with neuropathy (DN), and diabetic subjects with neuropathy and a history of ulceration (DNU) (58). Significantly higher forefoot peak plantar pressure was found in the DNU group (with mean around 415kPa) than that found in the normal (with mean around 330kPa). Significantly higher forefoot peak pressure gradient was also found in the DNU group

when compared to the normal (by 88%) and the DN group (by 44%). To reduce the risk of pressure ulcers in diabetic feet, custom-made contoured insoles are designed to more evenly distribute pressure over the plantar surface (59-61). It was found that contoured insoles cast in a semi-weight bearing condition can reduce the peak pressures, especially at the second and third metatarsal regions (61, 62). Studies were conducted to understand the effects of various types of insole materials and internal shoe structures on the plantar pressure distribution (63). Increase in heel height may shift the peak pressure region to the forefoot, such as to the first metatarsal and hallux regions (64). A rocker bottom outsole may reduce the forefoot pressure during walking (65).

Beside pressure, shear stresses acting on the plantar foot surface were also measured using biaxial or triaxial transducers discretely embedded in the insole (66-68). This allows monitoring of the shear stresses in two orthogonal directions dynamically. However, it is still difficult to have the full view of plantar shear distribution as only a limited number of transducers can be embedded in the insole due to the size of the transducer. Shear stress during normal walking was as high as 122kPa under the first and second metatarsal regions, and there was no significant difference between normal and diabetic subject groups (67). Shear stress up to 154kPa was recorded under the second metatarsal at pushoff during normal walking with a 3-inch high heeled shoe (68).

The temporal characteristics of plantar foot pressure and shear distribution were compared between diabetic patients with neuropathy and non-diabetic subjects during barefoot walking in (69). It was noted that the pressure-time integral and the resultant shear-time integral were increased by 54% and 132% respectively in the diabetic group when compared to the non-diabetic group.

4.3 Stresses at the Residual Limb / Prosthetic Socket Interface

The stress distribution at the interface between the residual limb and prosthetic socket is critical to socket design (70). The measurement techniques involve either inserting a thin sensor mat between the socket and skin, or positioning the transducers through the socket with the sensing surface leveled at the skin (71-76).

The pressures at the skin-socket interfaces reportedly vary widely among sites, individuals, and clinical conditions. For the Patellar-Tendon-Bearing (PTB) socket, the maximum peak pressure reportedly reached above 300kPa (72, 77-79). The wide variation may result from the diversity of prostheses and fitting techniques, the difference in residual limb geometry, site, soft tissues thickness, and time within the gait cycle.

Measurements of shear stresses at the residual limb/skin interfaces were first reported in (80). Triaxial transducers with small size were developed to monitor the pressure and shear stresses in two orthogonal directions and used for the interface stress measurements on below-knee sockets (71, 72). Interface shear stress ranging up to 57kPa was reported (78). Changes in socket-limb interface stress have been observed over time due to the changes in residual limb volume (78). Changes with different alignments (81), and with different kinds and styles of walking (79, 82) have been studied and reported. There was a 30% increase in interface pressure at the patella-bearing site during stair-climbing as compared to level walking (79).

5. HYPOTHESES FOR THE FORMATION OF PRESSURE ULCER

The mechanisms behind the abrasive ulcers that involve primarily superficial tissues are likely to be different from the mechanisms behind the deep tissue injuries near the bony prominences. Both mechanisms involve epidermal loadings. A major differentiating mechanism for the abrasive ulcers is presumably the presence of frictional rubbing between the skin surface and the body support surface.

There is an apparent inverse relationship between the pressure and its duration of application leading to the formation of pressure ulcers (83-85). There were attempts to interpret the inverse pressure-duration relationship biomechanically. The phenomenon was explained in terms of the interstitial fluid loss (86). By postulating that the pressure ulcer problem can be adequately described by the applied pressure, the duration of loading, tissue density, tissue modulus of elasticity, and tissue blood flow, it was predicted in a dimensional analysis that the allowable pressure p decreased with duration time t in the manner of $p \propto t^{-4/3}$ (87).

Quite a number of hypotheses have been proposed for the biomechanics of pressure ulcer in the past decades (88). The levels of evidence for those hypotheses vary. While some involved primarily circumstantial evidence and remained as mere speculations, some have attracted considerable attention over the years with related in-vivo and in-vitro findings becoming more available. They include (a) local ischemia and anoxia due to blood flow occlusion, (b) compromised lymphatic transports resulting in accumulation of toxic substances in the tissues, (c) reperfusion injuries concomitant with reactive hyperaemia, and (d) direct mechanical insults to cells causing cellular necrosis.

The hypothesis involving blood flow occlusion was among the earliest hypotheses made to explain the formation of pressure ulcer (89). When skin is compressed during daily activities, the underlying microvasculature can be affected. Short duration of compromises in blood supply usually does not affect the metabolism of skin and subcutaneous tissues. Sufficient magnitude of pressure can partially or totally arrest the circulation, which if prolonged, can result in tissue ischemia. It is reasonable to expect that no mammalian tissues can survive sustained ischemia indefinitely. Based on this hypothesis, it has been suggested that to avoid pressure ulcers, epidermal pressure should not exceed the typical capillary blood pressure of 4.3kPa, lest the microvasculature would collapse under external pressure and the supply of oxygen and nutrients to the tissues be compromised. Occlusion pressure for microvasculature actually varied with health conditions and sites (90-93). However, it has been documented that tissues can survive ischemia for duration much longer than those usually observed in pressure ulcer formation (94).

A sustainable environment for tissue survival not only depends on an adequate blood supply for timely transport of oxygen and nutrients, but also on an effective lymphatic system to remove the metabolic wastes and other toxins. Prolonged exposure of excessive epidermal loading can potentially compromise the lymphatic transports and allow such metabolic wastes and other toxins to accumulate in the tissues, causing ultimately cell death and tissue damage (95-97). Compared to the other hypotheses, this one has been less tested directly in previous studies on pressure ulcer.

Ischemic reperfusion has long been hypothesized to play a key role in the development of pressure ulcer (98-100). Ischemia-reperfusion injury is a major complication associated with many medical challenges, such as myocardial infarction, stroke, and

organ transplantation (101, 102). Reperfusion to ischemic tissues elevates the level of the highly reactive free radicals or molecules, which in excess can boost oxidative stress to an undesirable level, let loose inflammation, and lead to cell apoptosis and necrosis. They include highly reactive oxygen species such as superoxide radicals, and molecules like hydrogen peroxide. These reactive oxygen species are mostly generated in mitochondria-facilitated activities. They are also associated with inflammatory activities involving neutrophils and macrophages. During ischemia, xanthine oxidase (XO) accumulates in the hypoxic tissues. Hyperaemic reperfusion replenishes oxygen to these XO loaded ischemic tissues. The subsequent biochemical processes produce the high reactive superoxide and hydrogen peroxide, which can kick-off the oxidative damages. It was also known that nitric oxide (NO) can react with superoxide to form peroxynitrite, a reactive nitrogen specie with a relatively long half-life and able to damage cell membrane and protein structure (103). It is worth noting that oxidative stress is involved in nearly all inflammatory diseases (104). Hence, it may not be always easy to differentiate the ischemia-reperfusion responses from those of the post-compression responses, particularly when compression itself can result in a damage situation that calls for inflammatory responses.

Conceptually, it is not difficult to imagine that large enough epidermal mechanical insults can directly disrupt the involved tissues and damage the cells within them. Obvious examples include impact injuries in sports and vehicular accidents, as well as cuts and bruises. These injuries are associated with very high stresses applied onto the body surface. The question of course is whether the epidermal stresses at the body support surfaces, which are usually significantly lower than those associated with impacts and cuts, can disrupt the involved tissues and kill the cells inside when applied long enough.

Shear was noted quite early as a major contributor to the problem of pressure ulcer (105). Using a swine model, it was observed that frictional shear increased the susceptibility to skin breakdown at constant pressures of less than 67kPa (106). For pressure greater than 67kPa, frictional shear did not cause any additional ulceration. It was suggested that large gradient of normal stresses would produce shear deformation that can severely damage soft tissues (107). It was experimentally shown that the pressure necessary to produce blood occlusion at the Ischial tuberosities could almost be reduced by a factor of 2 when sufficient shear was developed at the seat-support interface (108, 109). It was remarked that about 40% of pressure ulcers are caused by shear injury (110). Skin blood flow in response to epidermal shear was studied using laser Doppler flowmetry (111). Skin blood flow was found reduced when either epidermal pressure or shear increased. It would be very useful to extend the pressure-duration tolerance curve systematically to include epidermal shear as well.

While the above pathophysiological mechanisms can all be induced in principle by prolonged excessive epidermal loadings, their exact roles and relative contributions to clinical pressure ulcers may vary. At the end of the day, the relevance of a hypothesis for the development of pressure ulcers must be evaluated in term of its power to explain the observations of clinical pressure ulcers. At a given epidermal loading, time is apparently a critical variable in pressure ulcer formation. It would be important to assess the relative contributions of all the major time-dependent processes involved, such as the viscoelastic deformational responses of the involved tissues, and the kinetics of all the relevant biological responses.

6. STUDIES ON TISSUE RESPONSES TO EPIDERMAL STRESSES

6.1 Tissue Deformation and Internal Stresses

It is important to understand how the forces externally applied on the skin affect the tissues internally, where blood circulation and cell functions can be influenced and pressure ulcers may initiate. Imaging techniques such as X-ray, ultrasound, CT and MRI have been used to obtain information on the involved internal structures (29), including tissue deformation and damage caused by external loading.

Ultrasound was used to study pressure ulcer development in human tissues over the heel, sacrum and ischial tuberosity (112). Superficial and deep tissue edema were readily differentiated. In about 79% of the images deemed abnormal, edema could be observed in the cutaneous and subcutaneous tissues before clinical erythema became apparent.

The role of ischemia and deformation in the onset of deep tissue pressure ulcer was studied in rats using a T2- weighted 6.3 Tesla MRI (113). Rat tibialis was either subjected to a 2-hrs indentation (yielding an epidermal pressure of about 150kPa and a maximum shear strain up to 1.0 internally) or a 2-hrs ischemia by applying a tourniquet proximally. During and immediately after indentation, tissue ischemia and reperfusion were respectively demonstrated using contrast-enhanced perfusion MRI. T2 value in the previously indented zone was visibly increased, indicative of tissue necrosis; whereas tissues with tourniquet-induced ischemia did not show such change. These results substantiated the claim that epidermal indentation of such magnitude was responsible

for the necrosis observed. A deformational threshold apparently existed beyond which damage increased with increasing maximum shear strain (114, 115).

An open-MR system (0.5 Tesla) was used to scan a seated subject to obtain the boundary displacements of the ischial tuberosity and the deformed buttock surface on the seating support (116). Using such boundary information, a computational model predicted that the highest principal compressive stress (32kPa) and strain (74%) occurred in the muscle layer rather than in the skin or subcutaneous fat. The predicted interface pressure (18kPa) under the ischial tuberosity matched well with the experimental measurement (17kPa). The internal peak stresses and strains were much higher among the paraplegics than the normal, mostly resulting from the anatomical differences in muscle thickness and the radius of curvature of the ischial tuberosity (117).

Such technique was used to predict real-time subcutaneous stresses from real-time interface stresses recorded experimentally. The internal stresses were reportedly 3 to 5 times higher in the buttock tissues of SCI subjects than in the normal during wheelchair sitting (118). By defining an internal stress relief event as when the peak compressive stress was below 2kPa for at least one second and by defining stress dose as the integral of peak compressive stress over time, the above method predicted a stress dose more than 30 times higher in SCI subjects than in normal. The number of internal stress relief events was about 10 times greater in normal than in SCI. The same MRI-computational approach with the experimentally measured interface conditions was applied to predict the internal stress and strain in residual limb tissues (119). A similar approach was adopted by combining X-ray anatomical measurements with insole-based interface measurements to predict the real-time internal stress and strain in heel pads

during walking (120). Maximum principal compressive stress as high as 500kPa and maximum Von Mises stress as high as 800 kPa were predicted.

Computational models in these studies are mainly based on finite element (FE) methods. Many FE models have been developed to assess internal stress and strain in tissues interacting with external body support surfaces, including the buttock / seating system (121), the plantar foot / insole system (122), and the residual limb / prosthetic socket system (123-125). The FE models varied in their degree of sophistication, depending on the purpose of the models. They could be grouped into three types. The first type involves linear static analysis established by assuming linear material properties, infinitesimal deformation and linear boundary condition without considering any interface friction and slip (123). The second type involves nonlinear analysis, taking into consideration nonlinear material properties, large deformation, and nonlinear boundary conditions, including friction/slip contact boundary (124). The third type are dynamic models, considering not only dynamic loads, but also material inertial effects and time-dependent material properties (125).

The accurate simulation of interactions between body tissue and support surface is challenging. Interface elements were introduced to simulate the friction/slip boundary condition (126-128). Special 4-node elements connecting the skin and the liner by corresponding nodes were used to simulate the friction/slip condition. An automated contact method was developed to simulate frictional slip at the socket/residual limb interface, in which correspondence between socket and limb was not required (129). Contact elastic bodies have been widely used for similar purpose (124, 125, 130, 131).

The average difference between interface stresses with and without considering inertia was 8.4% during stance phase and 20% during swing (125). The dynamic effect should be even bigger under impact loading.

Comprehensive 3D FE models of the human foot and ankle were developed, consisting of 28 bony structures, 72 ligaments and the plantar fascia embedded in a volume of encapsulated soft tissue. The model included large deformations and interface slip/friction conditions to study the interactions between the foot and supports (130). Hyper-elastic material properties were assigned to the encapsulated soft tissue and shoe sole. The models were used to study the sensitivity of design factors of foot orthosis on load transfer (122). Using similar modelling techniques, female foot models were developed to study the high-heeled shoe biomechanics (131).

The viscoelastic layer of skin and subcutaneous tissue on a bony substratum was modeled as a hydrated biphasic poroelastic layer (132, 133). This was used to interpret the threshold pressure-duration curve for pressure ulcer formation. Tissue compaction was suggested as a critical biomechanical field variable relevant to certain key biological response to prolonged mechanical loading. In a fluid-filled tissue matrix, tissue compaction builds up as interstitial fluid moves away from the loaded region. If tissue compaction reaches a critical value, direct cellular insults and/or microcirculation damage may result. It was noted that epidermal shear traction can largely reduce the time to achieve a certain tissue compaction and may quicken the formation of tissue ulcers. However, little direct experimental evidence has been reported on interstitial flows in the involved tissue systems.

6.2 Reperfusion and Flowmotion

In response to the compression-ischemia insult, blood flow re-entering the occlusion site is elevated and sustained to compensate for the oxygen debt caused earlier. In animal studies, ischemia reperfusion injury has been demonstrated in the context of pressure ulcers (92, 134-136). An adaptive effect of skin perfusion was reported in healthy subjects, where tissue oxygenation remained unaffected after a number of loading cycles. In contrary, subject with multiple sclerosis showed progressively diminishing tissue oxygenation with cyclic loading (137).

Laser Doppler Flowmetry (LDF) was applied to a rat trochanteric model to study skin perfusion responses to incremental epidermal pressure (3-min steps of 0.5kPa up to complete blood occlusion at about 7.7kPa) before and after prolonged loading of 12.2kPa for 5 hrs) (100). Before the prolonged loading, skin perfusion initially increased with epidermal pressure and then decreased when the epidermal pressure passed beyond 1.8kPa. Immediately after the prolonged loading, reactive reperfusion shot up to 3 times the normal value. After 3 hrs recovery, perfusion did not return to the original level but remained significantly higher. LDF spectral analysis showed that the magnitude of the low-frequency (< 1 Hz) response became lower after the prolonged loading, suggesting that the rhythmic vasodilatory mechanism was possibly compromised. When the stressed skin was subjected to the incremental epidermal pressure again, the initial phase of increasing perfusion with increasing pressure was lost. Subsequent repeated prolonged loading led a reactive reperfusion 45% lower than the first one.

The post-occlusion hyperaemic responses were investigated using a Laser Doppler Imager in human greater trochanteric tissues after three different types of loading,

namely static pressure alone (about 23kPa), a combination of static pressure and shear, and the combination of pressure and cyclic shear (138). Resting skin blood flow was higher in the normal as compared to the wheelchair users. The post-occlusive hyperaemic response was characterized by the peak hyperaemia, total hyperaemia (perfusion-time integral), and the hyperaemia half-life (time for peak hyperaemia to drop 50%) (Figure 2). In normal subjects, the peak and total hyperaemia after combined loading of pressure and cyclic shear was significantly higher than after the other two types of loading, and the hyperaemia half-life was longest for pressure plus cyclic shear. For wheelchair users, the peak hyperaemia was similar among the three loading conditions. However, both the hyperaemia half-life and total hyperaemia significantly increased when shear was introduced to the loading regimes. Arguably, one may interpret the initial reactive hyperaemic response as an indication of the severity of the earlier biomechanical insult. Using that perspective, these results seemed to support the hypothesis that a combination of epidermal pressure and shear stress cause a higher distress to the involved tissues than pressure alone and that dynamic loading could cause even higher distress to the tissues.

Disturbed flowmotion is another sign of tissue distress inducible by epidermal loading (139, 140). Flowmotion is the rhythmic oscillation in the vascular network due to contraction and dilation of the local smooth muscles (141). There was disturbed flowmotion at the sacrum in some SCI patients and elderly subjects in resting condition (139). The specific origins of such disturbance have not been fully understood. Wavelet analysis was applied to study the flowmotion signals in both time and frequency domains (142). Five characteristic frequencies have been identified in the human cutaneous circulation as recorded by LDF (142, 143). These oscillations reflect the influence of heart beat, respiration, intrinsic myogenic activity of the vascular smooth muscle,

neurogenic activity on the vessel wall and endothelial related metabolic activity with frequencies around 1, 0.3, 0.1, 0.04 and 0.01Hz, respectively (142, 144-146). The rhythmic flowmotion in the peripheral microcirculation in tissues overlying the ischial tuberosity (IT) in normal persons and persons with SCI were compared in (140). The relative amplitude of flowmotion at the frequency associated with endothelial related metabolic activities during resting condition was significantly lower in SCI than in normal. During the post-loading (16 KPa) period, the relative amplitude of the flowmotion at the frequency associated with neurogenic activities was evidently lower in SCI. These findings suggested that the contributions of endothelial related metabolic and neurogenic activities to the blood perfusion regulation was compromised in SCI individuals.

Most studies measured perfusion only within a few hundred microns from skin surface, and thus focused primarily on cutaneous microcirculation. By combining HeNe LDF and Photoplethysmography (PPG) with near-infrared, it is possible to measure perfusion covering a few thousand microns below surface. Bergstrand et al (147) used this technique to examine in normal subjects blood flows simultaneously at different depths over the sacrum, i.e. both cutaneous microcirculation and deeper blood flow in the muscles. Changes in circulatory responses were monitored before, during and after pressure loading up to 6.7kPa. PPG data revealed that at such low epidermal pressure, deeper blood flow in muscles often increased with epidermal loading, suggesting that in normal muscles, there may be a compensatory response to counteract the effects of the epidermal compression. It is interesting to note that reactive reperfusion was detected more often in the superficial tissues than in the deeper tissues.

6.3 Histological, Cellular and Molecular Studies

A pig model was used to examine how skin tissues responded to repetitive compressive and shear stresses at 1 Hz for 1 hour/day, 5 days/week for 4 weeks (148). The periodic stress waveform mimicked those typically experienced at the prosthetic socket/ residual limb interface. Histology showed a significant increase in collagen fibril diameter and a significant decrease in collagen fibril density, resulting in a similar collagen percentage over the dermal cross sectional area. Roughly similar trends of results were obtained in an in-vitro study on pig skin explants subjected to 30 minutes of stressing daily for 3 days (149). The in-vitro results were less substantial, possibly in part due to its being a shorter study.

Rat dorsal skin was subjected to prolonged cycles of loading-unloading with concomitant ischemia-reperfusion using an implanted ferromagnetic steel plate with an externally placed magnet (135). The magnet placed over the implanted plate generated a pressure of about 6.7 kPa in skin with a concomitant 80% reduction in blood flow. Tissue damages were documented in terms of area of tissue necrosis and number of extravasated leukocytes in the compressed zone. Tissue damages increased with number of loading-unloading cycles and total loading duration. More damages were observed in skins subjected to five cycles of loading (2 hrs) / unloading (0.5 hr) than those subjected to ten hours of continuous loading. Using a skinfold chamber in a mouse model (136), cyclic loading-unloading was applied to skin. Significantly more compromised microvasculature was observed in skins subjected to 4 cycles of loading (2 hrs) / unloading (1 hr) as compared to continuous loading for 8 hours. These studies clearly demonstrated the additional damages induced by reperfusion during the unloading phase.

A similar magnetic loading system was used to study in wild-type and transgenic mice how the loss of monocyte chemoattractant protein-1 (MCP-1) attenuated ischemia-reperfusion injury in skin (150). Ischemia-reperfusion injury was found closely associated with infiltration of macrophages and the release of highly reactive free radicals such as nitric oxide (NO), Tumor Necrosis Factor α (TNFα) and other proinflammatory cytokines. MCP-1 is recognized for its role in recruitment of macrophages and other inflammatory responses. Its level was significantly increased in wild-type mice after one cycle of loading (12 hrs) / unloading (12 hrs), together with elevated mRNA expression of inducible nitric oxide synthase (iNOS), TNFα, as well as other proinflammatory cytokines at various time points. Compared to the wild-type, MCP-$1^{-/-}$ mice showed less macrophage recruitment, earlier wound healing (possibly due to less skin injury), and significantly curbed mRNA expressions of iNOS and TNFα in the compressed skin. Furthermore, MCP-$1^{-/-}$ mice, unlike the wide-type, did not show much difference in the number of fibroblastic apoptotic cells, subsequent to 36 hours of continuous compression versus three cycles of the loading (12 hrs) / unloading (12 hrs) scheme. In case of the wild-type, such difference was more than 2-folds. This suggests that a significant proportion of reperfusion-induced apoptosis among cutaneous fibroblasts is MCP-1 facilitated.

It was generally understood that muscles could tolerate ischemia for a few hours (151). The molecular responses to ischemia-reperfusion of rat gastrocnemius muscle as a function of ischemic time was investigated by clamping the femoral blood vessel up to 6 hours (94). Histologically, interstitial edema was increasingly evident with time of reperfusion after 6 hours of ischemia. Extravasation of blood cells and leukocytes

infiltration were observed after 48 hours reperfusion, and muscle fibers fragmentation was also observed at 72 hours. The levels of p53, $p21^{WAF-1}$, and Bax did not change immediately after 6 hours of ischemia alone, but gradually increased subsequently and remained significantly elevated even after 72 hours subsequent to reperfusion when compared to the sham control. The accumulation of p53, $p21^{WAF-1}$ and Bax proteins are indicative of cellular responses to DNA damage, involving cell cycle arrest and apoptosis. The histological responses during reperfusion after 3 hours of ischemia were significantly milder, with the apoptotic signaling protein Bax showing no significant differences from the sham control. The results suggested that reperfusion injury after 3 hours of ischemia were more manageable compared to those after 6 hours of ischemia. It is interesting to note that ischemia itself for up to 6 hours before the subsequent reperfusion apparently did not cause significant changes in the histology nor in the p53, $p21^{WAF-1}$ and Bax levels.

The effects of reperfusion rates were studied in rat soleus muscle after 150 minutes of complete ischemia by clamping the femoral artery (152). A lower reperfusion rate was achieved by releasing the clamp gradually and monitoring the blood velocity in the process. Less histological damage and tissue oxidative stress markers (malonyldialdehyde and myeloperoxidase) in the gradual release group showed there was less reperfusion injury as compared to the fast release group.

It has been recognized that compared to skin, muscle tissue has a lower tolerance to lateral mechanical compression (1, 153-155). An in-vivo rat model was used to investigate the histological responses of skin and the subcutaneous tissues to 6 hours of pressure loading of 13.3 kPa per day at the greater trochanter and tibialis areas for up to 4 days (155). It was documented that such epidermal loading caused about 70% and

50% reduction of blood flow during compression in the trochanteric and tibialis areas respectively. Cutaneous tissue damage was observed at the trochanteric area after loading for two consecutive days but not noticeable after one day. Skin damage was evidenced by keratin layer thickening and fluid accumulation in the epidermis and seemed to persist even 3 days after the 4 days of loading. Such skin damage was not observed at the tibialis area for all time groups. However, muscle degeneration, as evidenced by increased number of centrally located nuclei in the muscle fibers, muscle fibers with rounded cross-sections and abnormal size variation, were observed after two consecutive days of loading at the tibialis. (Figure 3) Other histological damages included the internalization of peripherally located nuclei, replacement of muscle cells by fibrosis and adipose tissues, and the presence of pyknotic nuclei as well as karyorrhexis. Again, muscle damage was not noticeable after one day of such pressure loading, which appeared to be consistent with the observation in (156) on rat gracilis muscle subjected to 11.5kPa pressure for 6 hrs. However, at higher pressures (35kPa and 70kPa), extensive damage was reported *immediately* after the first day of loading. On the other hand, 50kPa pressure on pig trochanter for 2 hrs did not result in noticeable histopathological signs immediately upon cessation of loading (134). Histological signs of damage in subcutaneous tissues and muscles started to appear 1 hr after pressure cessation. Biochemical findings in blood hydrogen peroxide and in tissue glutathione apparently suggested a build-up of oxidative stress with reperfusion after loading. Severe muscle damage was observed histologically in rat tibialis anterior one hour after the muscle was subjected to a two hours indentation of ~4mm (corresponding to a pressure loading of about 150kPa) (154). Infiltration of polymorphonuclear neutrophils and monocyes was evident within 20 hours after the indentation. Phosphotungstic acid hematoxylin was used to demonstrate muscle damage by loss of cross-striation immediately after loading, thus minimizing the influence of reperfusion injury on the

histology (157). Substantial loss of cross-striation in gracilis muscle occurred just after 35kPa compression for 15 minutes. By combining results from different laboratories, a sigmoid type pressure-duration tissue tolerance curve was suggested for albino rats. Epidermal pressure above 32kPa tended to result in muscle damage even for very short exposure; whereas pressure below 5kPa apparently could be tolerated for much longer.

The same rat model was used to compare the results from compression with an indenter to those from complete ischemia using a tourniquet (113). Histological samples of the tibialis anterior were collected 4 hours after the removal of the indenter or the tourniquet. Two hours of indentation (corresponding to 150kPa pressure loading) apparently led to much more serious muscle damage than two hours of complete ischemia. These histological findings, collected 4 hours after the removal of the insult, likely also included the effects of the subsequent reperfusion injuries.

In vitro models allow the uncoupling of the damages caused by deformation and those by ischemia-reperfusion. The mechanical and failure properties of single C2C12 myoblasts were studied under compression (158). The average Young's modulus of the myoblasts was estimated to be around 1.14kPa. Lateral bulges started to appear at the cell membrane when axial strain reached about 60%, from where the compressed cell further stiffened until the cell membrane finally ruptured at about 72% strain, corresponding to an axial force of around 8.7μN.

To study the behavior of myoblasts in a 3-dimension construct, myoblasts were seeded in agarose gel and subjected to constant compression for various durations under a confocal microscope (159). At 10% axial construct strain, cell damage appeared to rise significantly after 2 hours as compared to the control. At 20% strain, 50% of the cells

were found damaged after 2 hrs as compared to the 30% plateau in the control, and after 24 hours at 20% strain, damage reached 100%.

Three-dimensional constructs of muscle myotubes in collagen gel was subjected to gross compressive strains of 30% and 50% (160). Compared to the control with only 4-5% cell death over time, constructs subjected to 30% and 50% axial strain showed an immediate jump of cell death to 8.2% and 13.6% respectively, as a direct damage of the cell membrane. Constructs at 30% strain showed a gradual increase in cell death percentage, reaching about 50% after 8 hrs, whereas constructs at 50% strain showed a much steeper rise, reaching about 75% cell death by hr-4 and the gradually reaching 80% by hr-8. The increase of cell death percentage with time under constant applied strain might reflect internal strain redistribution among the myotubes and within the viscoelastic cytoskeletal structures, the time-course of the apoptotic kinetics, and the interplay between the two. It is not clear how the in-vitro compressed myotubes may respond to the removal of the compression.

The relative contributions of compression (up to 40%) and hypoxia (down to 0%) to the development of muscle damage was studied in (161) using an in-vitro model of tissue-engineered muscle cells. Results from studies up to 22 hours indicated that hypoxia alone or superimposed on compression had relatively little effect on either muscle apoptosis or necrosis. These results are consistent with the in-vivo findings in (113), if hypoxia is taken to be a key consequence of ischemia.

By subjecting spherical indentation to the above tissue-engineered muscle cell construct (162), increasing diameter of the zone of cell deaths with time was observed using fluorescent propidium iodine under a confocal laser scanning microscope. Knowing the

strain field under the spherical indenter, a sigmoid type strain-time cellular tolerance curve was suggested. Construct compressive strain above 65% may be sufficient to result in cell damage even for very short exposure; whereas strain less than 35% may likely be tolerated for much longer period of time.

Changes in intracellular calcium during compression of individual myotubes in monolayer was studied using a calcium sensitive fluorescent probe (163). About half of the cells were unresponsive to incremental deformation, while the other half showed a brief calcium transient when subjected to a deformation increment of more than 30%. Ultimately, cell necrosis was consistently accompanied by a steep up-regulation of intracellular calcium, likely indicative of an irreversible disruption of cell membrane. When happened, some of the surrounding viable cells were also similarly affected.

In a similar rat model used in (155), it was demonstrated that 6 hours of prolonged pressure of 13.3 KPa per day for 2 days was enough to activate apoptosis in the subcutaneous muscle tissue (164). The study showed that under moderate epidermal loading, there were increases in the transcript content of caspase-8 , Bax and Bcl-2, as well as an enhanced activation of downstream caspase-3 activities. These caspase-8 and capspace-9 /Bcl-2 family proteins correspond respectively to the death receptor-mediated and mitochondria-mediated apoptotic pathways. These results suggested that the two pathways may both be involved in pressure-induced apoptosis, and together help to amplify the deep tissue damage.

7. CLOSING REMARKS AND SUGGESTIONS FOR FUTURE RESEARCH

Ischemia has long been hypothesized as a key mechanism for pressure ulcer formation. Pure ischemia for a few hours without compression may not immediately cause histological signs of muscle damage. The molecular cascade of ischemia injury could have been triggered before histological changes show up. There is evidence that immediate muscle damage can occur as a direct mechanical insult under high enough loading. Damages can further build-up upon unloading, possibly due to subsequent reperfusion oxidative stresses and inflammation responses. Such loading-unloading responses, if not appropriately relieved, can render the involved tissues more vulnerable to subsequent loadings, a process of damage accumulation in compromised body tissues interacting with external forces. Can the reperfusion-induced and inflammation-induced oxidative environment make cells more vulnerable to subsequent mechanical stresses and if so, how? Would epidermal keratinocytes, dermal fibroblasts, subcutaneous fat and muscle cells behave differently in response to oxidative stress?

What kinds of tissue adaptation may strengthen the tissues system to better withstand the epidermal loading? Tissue adaptation to epidermal loading can occur in skin when external pressure and shear were applied at levels below those known to cause tissue breakdowns. Thickening of plantar foot skin in response to epidermal pressure and shear can become pathological corns and calluses if not properly taken care of. Muscle stiffening has been reported in association with muscle injury, which was included in a damage law to describe how damage may expand from the deep muscle towards the skin surface (165). Development of these damage laws requires detailed understanding of the damage kinetics at the cellular and molecular level.

The same kind of tissues at different anatomical sites can have very different biomechanical tolerance. Are those differences experienced at the cellular level? How would the cells in buttock tissues differ from those in the heel? Can cells in the buttock tissues acquire the characteristics of cells in the heel pads, and if so, how?

Loading-duration tolerance curves were presented as pressure (or strain) - time curves for different anatomical sites and animals. To help understand the behaviour of the whole tissue systems, tolerance curves should be determined separately for skin, fat and muscle at the tissue and cellular levels. It would be clinically relevant if epidermal shear can be incorporated into such tolerance curves. What damage mechanisms are induced by shear as compared to pressure? If ischemia is the common mechanism, we may expect a similar molecular cascade to follow. If different cytoskeletal mechanisms are involved, the associated molecular events would be more different.

Reperfusion damage should be explicitly included in assessing tissue tolerance, by taking the loading-unloading cycle as a unit responsible for pressure ulcer formation. Besides knowing the capacity of a tissue to tolerate one loading episode, it is meaningful to know the sustainability of certain loading-unloading patterns. After all, loading and unloading always come back-to-back in real situation.

Few theoretical damage models have been proposed to simulate the time-dependent process of pressure ulcer formation. The time-dependent process has been modelled based on (a) tissue consolidation as fluid moves out of the tissue matrix under epidermal loading (132); (b) the empirical pressure-duration tolerance curve and the expansion of a stiffened zone of damaged muscle fibres (165); and (c) accumulation of cellular damage

as a result of hypoxia due to compression-compromised oxygen diffusivity (166). The process of reperfusion injury should also be included in the future damage models.

We stand, walk, sit and lie on surfaces most of the day. It is interesting that normal individuals can routinely cope with those forces without difficulty. Challenges occur when pathologies arise and/or when these external forces are redirected to unprepared/ unaccustomed tissues. One of the biggest challenges is that most of these external forces are quite unavoidable if the affected individuals are to continue to move and function in gravity. The problems are how to minimize these external forces during locomotion and various functions, how to distribute them more evenly over tolerant areas in space, and how to engage alternately in time the different support surfaces, so that these unavoidable loading and unloading cycles can be managed by our body tissues in a sustainable manner.

FIGURE CAPTIONS

Figure 1 Positions of ischial tuberosities and their corresponding peak pressures on pressure map during dynamic wheelchair propulsion (one normal subject). The peak pressure locations are anterior to the locations of the ischial tuberosities.

Figure 2 Schematic representation of a reactive hyperaemic response.

Figure 3 Photomicrograph of muscle fibres at the tibialis area. (155) (A) Normal muscle architecture of control rat shows closely packed polygonal muscle fibre profiles. There is little variation in muscle fibre size or shape. Cytoplasmic staining is uniform. Small, peripherally located nuclei are abundant. (B) Muscle fibres at 48hr, degeneration of muscle cells is characterized by increasingly numerous nuclei, which occupy the central part of the muscle fibres. (C) At 72hr, atrophic and hypertrophic muscle fibres with round contours are present. (D) At 96hr, muscle fibres are replaced by fibro-fatty tissue, with abnormal variation in fibre size due to atrophy of some and hypertrophy of others. (E) At 96hr, muscle fibres become necrotic. Peripherally located nuclei of muscle fibres become internalized. There is destruction of muscle fibres with replacement of the muscle by fibrous tissue. (F) At 168hr, muscle fibres become severely necrotic, where muscle atrophy affects groups of muscle fibres supplied by single motor units in contrast to the haphazard pattern of atrophy seen at other groups. (H&E, x30)

REFERENCES

1. Daniel RK, Priest DL, Wheatley DC. 1981. Etiology factors in pressure ulcers: an experimental model. *Arch. Phys. Med. Rehabil*. 62:492-498.

2. Byrne DW, Salzberg CA. 1996. Major risk factors for pressure ulcers in the spinal cord disabled: a literature review. Spinal Cord 34:255-263.

3. Sumiya T, Kawamura K, Tokuhiro A, Takechi H, Ogata H. 1997. A survey of wheelchair use by paraplegic individuals in Japan. part 2: prevalence of pressure ulcers. *Spinal Cord* 35:595-598.

4. Brand PW. 1979. Management of the insensitive limb, *Physical Therapy* 59:8-12.

5. Boulton AJM, Betts RP, Franks CI. 1987. Abnormalities of foot pressure in early diabetic neuropathy. *Diabetic Medicine* 4:225-228.

6. Pecoraro RE, Reiber GE, Burges, EEM. 1990. Pathways to diabetic limb amputation: basis for prevention. *Diabetes Care* 13:513-521.

7. Levy SW. 1980. Skin problems of the leg amputee. *Prosthet. Orthot. Int*. 4:37-44.

8. Nielsen CC. 1990. A survey of amputees: functional level and life satisfaction, information needs, and prosthetist's role. *J. Prosthet. Orthot*. 3:125-129.

9. Lyon CC, Kulkarni J, Zimerson E, Van Ross E, Beck MH. 2000. Skin disorders in amputees. *J. Am. Acad. Dermatol*. 42:501-507.

10. Reddy M, Gill SS, Kalkar SR, Wu W, Anderson PJ, Rochon PA. 2008. Treatment of pressure ulcers: a systematic review. *J. Am. Med. Assoc*. 300:2647-2662.

11. Kanitakis J. 2002. Anatomy, histology and immunohistochemistry of normal human skin. *European Journal of Dermatology* 12:390-401.

12. Brown IA. 1973. A scanning electron microscope study of the effects of uniaxial tension on human skin. *British Journal of Dermatology* 89: 383-393.

13. Lumpkin EA, Caterina MJ. 2007. Mechanisms of sensory transduction in the skin. *Nature* 445:858-865.

14. Kirk JE, Chieffi M. 1962. Variation with age in elasticity of skin and subcutaneous tissue in human individuals, *J. Gerontol*. 17:373-80.

15. Hall DA, Blackett AD, Zajac AR, Switala S, Airey CM. 1981. Changes in skinfold thickness with increasing age. *Age and Ageing* 10:19-23.

16. Ziegert JC, Lewis JL. 1978. In-vivo mechanical properties of soft tissues covering bony prominences*. ASME J. Biomech. Eng.* 100:194-201.

17. Barbenel JC, Payne PA. 1981. In vivo mechanical testing of dermal properties. In *Bioengineering and the Skin*, ed. R Marks, PA Payne, pp. 8-38. Lancaster: MTP Press.

18. Dikstein S and Hartzshtark A. 1981. In vivo measurement of some elastic properties of human skin. In *Bioengineering and the Skin*, ed. R Marks, PA Payne, pp. 45-53. Lancaster: MTP Press.

19. Bader DL, Bowker P. 1983. Mechanical characteristics of skin and underlying tissues in vivo, *Biomaterials* 4:305-308.

20. Malinauskas M, Krouskop TA, Barry PA. 1989. Noninvasive measurement of the stiffness of tissue in the above-knee amputation limb. *J. Rehabil. Res. & Dev*. 26:45-52.

21. Lanir Y, Dikstein S, Hartzshtark A, Manny V. 1990. In-vivo indentation of human skin. *ASME J. Biomech. Eng*. 112: 63-69.

22. Mak AFT, Liu GHW, Lee SY. 1994. Biomechanical assessment of below-knee residual limb tissue. *J. Rehabil. Res. & Dev*. 31:188-198.

23. Vannah WM, Childress DS. 1996. Indentor tests and finite element modeling of bulk muscular tissue in vivo. *J. Rehabil. Res.& Dev*. 33:239-252.

24. Zheng YP, Mak AFT. 1996. An ultrasound indentation system for biomechanical properties assessment of soft tissues in-vivo. *IEEE Trans. on Biomed. Eng.* 43: 912-918.

25. Pathak AP, Silver-Thorn B, Thierfelder CA, Prieto TE. 1998. A rate-controlled indentor for in vivo analysis of residual limb tissues. *IEEE Trans Rehabil Eng*. 6:12-20.

26. Zheng YP, Mak AFT, 1999. Effective elastic properties for lower limb soft tissues from manual Indentation experiment. *IEEE Trans. on Rehab. Eng*. 7:257-267.

27. Zheng YP, Mak AFT. 1999. Extraction of quasilinear viscoelastic parameters for lower limb soft tissues from manual indentation experiment. *ASME J. Biomech. Eng.* 121: 330-339.

28. Zheng YP, Choi YKC, Wong K, Chan S, Mak AFT. 2000. Biomechanical assessment of plantar foot tissue in diabetic patients using an ultrasound indentation system. *Ultrasound in Med & Biol.* 26:451-456.

29. Zheng YP, Mak AFT, Zhang M, Leung AKL. 2001. State-of-the-art methods for residual limb assessment: a review. *J. Rehab. Res. & Dev.* 38:487-504.

30. Gefen A, Megido-Ravid M, Itzchak Y. 2001. In-vivo biomechanical behaviour of human heel pad during the stance phase of gait. *J. Biomech*. 34:1661-1665.

31. Erdemir A, Viveiros ML, Ulbrecht JS, Cavanagh PR. 2006. An inverse finite-element model of heel pad indentation. *J. Biomech*. 39:1279-1286.

32. Then C, Menger J, Benderoth G, Alizadeh M, Vogl TJ, Hübner F, Silber G. 2007. A method for a mechanical characterization of human gluteal tissue. *Technology and Health Care* 15:385–398.

33. Makhsous M, Venkatasubramanian G, Chawla A, Pathak Y, Priebe M, Rymer WZ, Lin F. 2008. Investigation of soft-tissue stiffness alteration in denervated human tissue using an ultrasound indentation system. *J Spinal Cord Med*. 31:88-96.

34. Burbridge BE. 2007. Computed tomographic measurement of gluteal subcutaneous fat thickness in reference to failure of gluteal intramuscular injections. *Canadian Association of Radiologists Journal* 58:72-75.

35. Linder-Ganz E, Shabshin N, Itzchak Y, Yizhar Z, Siev-Ner I, Gefen A. 2008. Strains and stresses in sub-dermal tissue of the buttocks are greater in paraplegics than in healthy during sitting. *J of Biomech*. 41:567-580.

36. Todd BA, Thacker JG. 1994. Three dimensional computer model of the human buttock in vivo. *J Rehab. Res. & Dev*. 31:111-119.

37. Gefen a, Gefen N, Linder-Ganz E, Marqulies SS. 2005. In vivo muscle stiffening under bone compression promotes deep tissue sores. *ASME J Biomech. Eng*. 127:512-524.

38. Lemmon D, Shiang AH, Ulbrecht JS, Cavanagh PR. 1997. The effect of insoles in therapeutic footwear—a finite element approach. *J. Biomech*. 30:615-620.

39. Miller-Young JE, Duncan NA, Baroud G. 2002. Material properties of the human calcaneal fat pad in compression experiment and theory. *J Biomech.* 35;1523-1531.

40. Gooding GAW, Stess RM, Graf PM. 1986. Sonography of the sole of the foot, evidence for loss of foot pad thickness in diabetes and its relationship to ulceration of the foot, *Invest. Radiol*. 21:45-48.

41. Childress DS, Steege JW. 1987. Computer-aided analysis of below-knee socket pressure. *J Rehab. Res. & Dev.* 2: 22-24.

42. Reynolds DP, Lord M. 1992. Interface load analysis for computer-aided design of below-knee prosthetic sockets. *Med & Biol Eng & Comput*. 30:419-426.

43. Tonuk E, Silver-Thorn MB. 2003. Nonlinear elastic material properties estimation of lower extremity residual limb tissues*, IEEE Trans. Neural Sys. & Rehab. Eng*. 11: 43-53.

44. Allen V, Ryan DW, Lomax N. Murray A. 1993. Accuracy of interface pressure measurement systems. *J Biomed Eng.*15:344–348.

45. Ferguson-Pell MW, Cardi MD. 1993. Prototype development and comparative evaluation of wheelchair pressure mapping system. *Assist. Technol*. 5:78–91.

46. Buis A, Convery P. 1997. Calibration problems encountered while monitoring stump/socket interface pressures with force sensing resistors: techniques adopted to minimise inaccuracies. *Prosthet. Orthot. Int.* 21:179–182.

47. Pipkin L and Sprigle S. 2008. Effect of model design, cushion construction and interface pressure mats on interface pressure and immersion. *J. Rehabil. Res. & Dev.* 45:875-882.

48. Goossens RH, Snijders CJ, Holscher TG, Heerens WC, Holman AE. 1997. Shear stress measured on beds and wheelchairs. *Scand. J. Rehabil. Med.* 29:131–136.

49. Sprigle S, Dunlop W, Press L. 2003. Reliability of bench tests of interface pressure. *Asst. Technol.* 15:49-57.

50. Bogie K, Wand X, Fei B, Sun J. 2008. New technique for real-time interface pressure analysis: Getting more out of large image data sets. *J. Rehab. Res. & Dev.* 45(4):523-536.

51. Dabnichki P, Taktak D. 1998. Pressure variation under the ischial tuberosity during a push cycle. *Med. Eng. Phys.* 20:242-256.

52. Kernozek TW, Lewin JE. 1998. Seat interface pressure of individuals with paraplegia: influence of dynamic wheelchair locomotion compared with static seated measurements. *Arch. Phys. Med. Rehab.* 79:313-316.

53. Tam EW, Mak AF, Lam WN, Evans JH, Chow YY. 2003. Pelvic movement and interface pressure distribution during manual wheelchair propulsion. *Arch. Phys. Med. Rehab.* 84:1466-1472.

54. Lord M. 1981. Foot pressure measurement: a review of methodology. *J Biomed Eng,* 3: 91-99.

55. Cavanagh PR, Hewitt FG, Perry JE. 1992. In-shoe plantar pressure measurement: a review, *The Foot* 2:185-194.

56. Urry S. 1999. Plantar pressure-measurement sensors, Meas. Sci. Technol, 10:R16-R32.

57. Morag E, Cavanagh PR. 1999. Structural and functional predictors of regional peak pressures under the foot during walking. *J Biomech.* 32:359-370.

58. Lott DJ, Zou D, Mueller MJ. 2008. Pressure gradient and subsurfacwe shear stress on the neuropathic forefoot. *Clin. Biomech*. 23:342-348.

59. Lord M, Hosein R. 1994. Pressure redistribution by molded inserts in diabetic footwear: a pilot study, J. Rehab. Res. & Dev. 31:214-221.

60. Kato H, Takada T, Kawamura T, Hotta N, Torii S. 1996. The reduction and redistribution of plantar pressure using foot orthosis in diabetic patients, *Diabetes Research and Clinical Practice* 31: 115-118.

61. Tsung BYS, Zhang M, Mak AFT and Wong MWN. 2004. Effectiveness of insoles on plantar pressure redistribution*, J. Rehab. Res. & Dev*. 41:767-774.

62. Tsung YS, Zhang M, Fan YB, Boone DA. 2003. Quantitative Comparison of Plantar Foot Shapes under Different Weight Bearing Conditions, *J. Rehab. Res. & Dev*. 40:517-26.

63. McPoil TG, Cornwall MW 1992. Effect of insole materials on force and plantar pressures during walking. *J. Am. Podiatr. Med. Assoc.* 82:412-416.

64. Mandato MG, Nester E. 1999. The effects of increasing heel height on forefoot peak pressure. *J. Am. Podiatr. Med. Assoc.* 89:75-80.

65. Praet SF, Louwerens JW. 2003. The influence of shoe design on plantar pressures in neuropathic feet. *Diabetes Care* 26:441-445.

66. Tappin JW, Robertson KP. 1991. Study of the relative timing of shear forces on the sole of the forefoot during walking. *J. Biomed. Eng.*13:39-42.

67. Lord M, Hosein R. 2000. A study of in-shoe plantar shear in patients with diabetic neuropathy. *Clin. Biomech.* 15:278-283.

68. Cong Y, Luximon Y, Zhang M. 2009. Plantar pressure and shear stress in high-heeled shoes, *Proc. WACBE World Congress on Bioengineering*, Hong Kong, pp232.

69. Yavuz M, Tajaddini A, Botek G, Davis BL. 2008. Temporal characteristics of plantar shear distribution: relevance to diabetic patients. *J Biomech*. 41:556-559.

70. Mak AFT, Zhang M, Boone D. 2001. State-of-the-art Research in Lower Limb Prosthetic Biomechanics - Socket Interface. *J. Rehab. Res. & Dev.* 38:161-173.

71. Williams RB, Porter D, Roberts VC. 1992. Triaxial force transducer for investigating stresses at the stump/socket interface*. Med. & Biol. Eng. & Comput*. 1: 89-96.

72. Sanders JE, Daly CH. 1993. Measurement of stresses in the three orthogonal direction at the residual limb-prosthetic socket interface*. IEEE Trans. Rehab. Eng*. 12:79-85.

73. Lee VSP, Solomonidis SE, Spence. WD. 1997. Stump-socket interface pressure as an aid to socket design in prostheses for trans-femoral amputees – a preliminary study. *J. of Eng. in Med.* 211:167-80.

74. Zhang M, Turner-Smith AR, Tanner A, Roberts VC. 1998. Clinical investigation of the pressure and shear stress on the trans-tibial stump with a prosthesis. *Med. Eng. Phys*. 20:188-198.

75. Goh JCH, Lee PVS, Chong SY. 2003. Stump/socket pressure profiles of the pressure cast prosthetic socket, *Clin. Biomech.*, 18:237-243.

76. Polliack AA, Sieh RC, Craig DD, Landsberger S, McNeil DR, Ayyappa E. 2000. Scientific validation of two commercial pressure sensor systems for prosthetic socket fit. *Prosthet. Orthot. Int.* 24:63-73.

77. Meier RH, Meeks ED, Herman RM. 1973. Stump-socket fit of below-knee prostheses: comparison of three methods of measurement. *Arch. Phys. Med. Rehab*. 54:553-558.

78. Sanders JE, Zachariah SG, Jacobsen AK, Ferguson JR. 2005. Changes in interface pressures and shear stresses over time on trans-tibial amputee subjects ambulating with prosthetic limbs: comparison of diurnal and six-month differences. *J. Biomech*. 38:1566-1573.

79. Dou P, Jia XH, Suo SF, Wang RC, Zhang M. 2006. Pressure distribution at the stump/socket interface in transtibial amputees during walking on stairs, slope and non-flat road, *Clin Biomech,* 21:1067-1073.

80. Appoldt FA, Bennett L, Contini R. 1970. Tangential pressure measurement in above-knee suction sockets. *Bull. Prosthet. Res.* Spring:70-86.

81. Jia XH, Suo SF, Meng F, Wang RC. 2008. Effects of alignment on interface pressure for transtibial amputee during walking. Disability and rehabilitation. *Assistive Technology* 3:339-343.

82. Sanders JE, Zachariah SG, Baker AB, Greve JM, Clinton C. 2000. Effects of changes in cadence, prosthetic componentry, and time on interface pressures and shear stresses of three trans-tibial amputees. *Clin. Biomech*. 15:684-694.

83. Groth KE. 1942. Clinical observations and experimental studies on the origin of decubitus ulcers. Acta. Chir. Scand. 87(Suppl.76).

84. Kosiak M. 1961. Etiology of decubitus ulcers. Arch. Phys. Med. Rehab. 42:19-29.

85. Reswick JB, Rogers J. 1976. Experience at Rancho Los Amigos Hospital with devices and techniques to prevent pressure ulcers. In Bed Ulcer Biomechanics, ed. RM Kenedi, JM Cowden, JT Scales, pp.301-310. London: McMillan.

86. Reddy NP, Cochran GVB, Krouskop TA. 1981. Interstitial fluid flow as a factor in decubitus ulcer formation. J Biomech. 14:879-881.

87. Sacks AH. 1989. Theoretical prediction of a time-at-pressure curve for avoiding pressure ulcers. J. Rehab. Res. & Dev. 26:27-34.

88. Bader D, Bouten C, Colin D, Oomens C. 2005. *Pressure ulcer research: current and future perspectives*. Berlin: Springer.

89. Murno D. 1940. Care of the back following spinal-cord injuries: a consideration of bed ulcers. *New Engl. J. Med.* 223:391-398.

90. Barnett RI, Ablarde JA. 1994. Skin vascular reaction to standard patient positioning on a hospital mattress. *Adv. Wound Care* 7:58-65.

91. Wang WZ, Anderson G, Firrell JC, Tsai TM. 1998. Ischemic preconditioning versus intermittent reperfusion to improve blood flow to a vascular isolated skeletal muscle flap of rats. *J. Trauma* 45:953-959.

92. Sundin BM, Hussein MA, Glasofer S, El-Falaky MH, Abdel-Aleem SM, Sachse RE, Klitzman B. 2000. The role of allopurinol and deferoxamine in preventing pressure ulcers in pigs. *Plast. Reconstr. Surg.* 105:1408-1421.

93. Baldwin KM. 2001. Transcutaneous oximetry and skin surface temperature as objective measures of pressure ulcer risk. *Adv. Skin Wound Care* 14:26-31.

94. Hatoko M, Tanaka A, Kuwahara M, Satoshi Y, Lioka H, Niitsuma K. 2002. *Annals of Plastic Surgery* 48:68-74.

95. Krouskop TA. 1983. A synthesis of the factors that contribute to pressure ulcer formation. *Medical Hypotheses* 11:255-267.

96. Miller GE, Seake JL. 1987. The recovery of terminal lymph flow following occlusion. *J. Biomed. Eng*. 109:48-54.

97. Reddy NP. 1990. Effects of mechanical stresses on lymph and interstitial fluid flow. In *Pressure Ulcers: Clinical Practice and Scientific Approach, ed.* DL Bader, pp203-222. London:Macmillan.

98. Bulkley GB. 1987. Free radical-mediated reperfusion injury: a selected review. *Br. J. Cancer.* 55(Suppl. VIII):66-73.

99. Granger DN. 1988. Role of xanthine oxidase and granulocytes in ischemia reperfusion injury. *Am. J. Physiol.* 255:H1269-H1275.

100. Herrman EC, Knapp CF, Donofrio JC, Salcido R. 1999. Skin perfusion responses to surface pressure-induced ischemia: implication for the developing pressure ulcer. *J. Rehab. Res. & Dev.* 36:109-120.

101. Clavien PA, Yadav S, Sindram D, Bentley RC. 2000. Protective effects of ischemic preconditioning for liver resection performed under inflow occlusion in humans. *Ann. Surg.* 232:155-162.

102. Collard CD, Gelman S. 2001. Pathophysiology, clinical manifestations, and prevention of ischemia-reperfusion injury. *Anesthesiology* 94:1133-1138.

103. Tayor R, James T. 2005. The role of oxidative stress in the development and persistence of pressure ulcers. In *Pressure Ulcer Research*, ed. DL Bader, C Bouten, D Colin, C Oomens , pp205-232. Berlin: Springer.

104. McCord JM. 2000. The evolution of free radicals and oxidative stress. *Am. J. Med.* 108:652-659.

105. Reichel SM. 1958. Shearing force as a factor in decubitus ulcers in paraplegics, *JAMA* 166:762.

106. Dinsdale SM. 1974. Decubitus ulcers: role of pressure and friction in causation*. Arch. Phys. Med. Rehab.* 55:147-152.

107. Bennett L. 1972. Part III: Analysis of shear stress. *Bull. Prosthet. Res*. 10:38-51.

108. Bennett L, Kavner D, Lee BK, Trainor FA. 1979. Shear vs pressure as causative factors in skin blood flow occlusion. *Arch. Phys. Med. Rehab*. 60:309-314.

109. Rowland J. 1993. Pressure ulcers: a literature review and a treatment scheme. Aust. Fam. Physician 22:1822-1827.

110. Bennett L, Lee BY. 1988. Vertical shear existence in animal pressure threshold experiments. *Decubitus* 1:18-24.

111. Zhang M, Roberts VC. 1993. The effect of shear forces externally applied to skin surface on underlying tissues. *J Biomed. Eng.* 15:451-456.

112. Quintavalle PR, Lyder CH, Mertz PJ, Phillips-Jones C, Dyson M. 2006. Use of high-resolution, high-frequency diagnostic ultrasound to investigate the pathogenesis of pressure ulcer development. *Adv in Skin & Wound Care* 19: 498-505.

113. Stekelenburg A, Strijkers GJ, Parusel H, Bader DL, Nicolay K, Oomens CW. 2007. Role of ischemia and deformation in the onset of compression-induced deep tissue injury: MRI-based studies in a rat model. *J. Appl. Physiol.* 102:2002-2011.

114. Ceelen KK, Stekelenburg A, Loerakker S, Strijkers GJ, Bader DL, Nicolay K, Baaijjens FPT, Oomens CWJ. 2008. Compression-induced damage and internal tissue strains are related. *J. Biomech.* 41:3399-3404.

115. Ceelen KK, Stekelenburg A, Mulders JLJ, Strijkers GJ, Baaijjens FPT, Nicolay K, Oomens CWJ. 2008. Validation of a numerical model of skeletal muscle compression with MR tagging: a contribution to pressure ulcer research. *ASME J. Biomech. Eng*. 130:061015-1 – 061015-8.

116. Linder-Ganz E, Shabshin N, Itzchak Y, Gefen A. 2007. Assessment of mechanical conditions in a sub-dermal tissues during sitting: a combined experimental-MRI and finite element approach. *J Biomech*. 40:1443-1454.

117. Linder-Ganz E, Shabshin N, Itzchak Y, Yizhar Z, Siev-Ner I, Gefen A. 2008. Strains and stresses in sub-dermal tissues of the buttocks are greater in paraplegics than in healthy during sitting. *J Biomech*. 41:567-580.

118. Linder-Ganz E, Yarnitzky G, Yizhar Z, Siev-Ner I, Gefen A. 2009. Real-time finite element monitoring of sub-dermal tissue stresses in individuals with spinal cord injury: towards prevention of pressure ulcers. *Ann. Biomed. Eng.* 37:387-400.

119. Portnoy S, Yizhar Z, Shabshin N, Itzchak Y, Kristal A, Dotan-Marom Y, Siev-Ner I, Gefen A. 2008. Internal mechanical conditions in the soft tissues of a residual limb of a trans-tibial amputee. *J. Biomech*. 41:1897-1909.

120. Yarnitzky G, Yizhar Z, Gefen A. 2006. Real-time subject-specific monitoring of internal deformations and stresses in the soft tissues of the foot: a new approach in gait analysis. *J. Biomech*. 39:2673-2689.

121. Grujicic M, Pandurangan B, Arakere G, Bell WC, He T, Xie X. 2009. Seat-cushion and soft-tisue material modeling and a finite element investigation of the seating comfort for passenger-vehicle occupants. *Materials and Deign* 30:4273-4285.

122. Cheung JTM, Luximon A, Zhang M. 2008. Parametrical design of pressure-relieving foot orthoses using statistical-based finite element method. *Med. Eng. Phys.* 30:269-277.

123. Zhang M, Mak AFT, Roberts VC. 1998. Finite element modelling of lower-limb / prosthetic socket - a survey of the development in the first decade. *Med. Eng. Phys.* 20:360-373.

124. Lee WCC, Zhang M, Jia XH, Cheung JTM. 2004. Finite element modeling of contact interface between trans-tibial residual limb and prosthetic socket. *Med. Eng. Phys*. 26:655-662.

125. Jia XH, Zhang M, Lee WCC. 2004. Load transfer mechanics between trans-tibial prosthetic socket and residual limb—dynamic effects. *J. Biomech*. 37) 1371-1377.

126. Zhang M, Lord M, Turner-Smith AR, Roberts VC. 1995. Development of a nonlinear finite element modelling of the below-knee prosthetic socket interface. *Med. Eng. Phys*. 17: 559-66.

127. Zhang M, Turner-Smith AR, Roberts VC, and Tanner A, 1996. Frictional action at residual limb/prosthetic socket interface. *Med. Eng. Phys*. 18:207-214.

128. Zhang M, Mak AFT. 1996. A finite element analysis of the load transfer between an above-knee residual limb and its prosthetic socket - the roles of interface friction and the distal-end boundary conditions. *IEEE Trans Rehab. Eng*. 4:337-346.

129. Zachariah SG, Sanders JE. 2000. Finite element estimates of interface stress in the trans-tibial prosthesis using gap elements are different from those using automated contact. *J. Biomech.* 33:895-899.

130. Cheung JTM, Zhang M, Leung AKL and Fan YB. 2005. Three-dimensional finite element analysis of the foot during standing - a material sensitivity study. *J. Biomech*. 38:1045-1054.

131. Yu J, Cheung JTM, Fan YB, Zhang Y, Leung AKL, Zhang M. 2008. Development of a finite element model of female foot for high-heeled shoe design, *Clin. Biomech*. 23:s31-s38.

132. Mak AFT, Huang LD, Wang QQ. 1994. A biphasic poroelastic analysis of the flow dependent subcutaneous tissue pressure and compaction due to epidermal loadings - Issues in pressure ulcer. *ASME J. Biomech. Eng, Trans.* 116:421-429.

133. Zhang JD, Mak AFT, Huang LD. 1997. A large deformation biomechanical model for pressure ulcers. *ASME J. Biomech. Eng*. 119:406-408.

134. Houwing T, Overgoor M, Kon M, Janen G, Van Asbeeck BS, Haalboom JRE. 2000. Pressure-induced skin lesions in pigs: reperfusion injury and the effects of vitamin E. *J Wound Care* 9:36-40.

135. Peirces SM, Skalak TC, Rodeheaver GT. 2000. Ischemia-reperfusion injury in chronic pressure ulcer formation: a skin model in the rat. *Wound repair and Regeneration* 8:68-76.

136. Tsuji S, Ichioka S, Sekiya N, Nakatsuka T. 2005. Analysis of ischemia-reperfusion injury in a microcirculatory model of pressure ulcers. *Wound Repair Regen.* 13:209-215.

137. Bader DL. 1990. The recovery characteristics of soft tissues following repeated loading. *J. Rehabil. Res. & Dev.* 27:141-150.

138. Mak AFT, Tam EWC, Tsung BYS, Zhang M, Zheng YP, Zhang JD. 2003. Biomechanics of body support surfaces: issues of decubitus ulcer. In *Frontiers in Biomedical Engineering*, ed. NHC Hwang, SLY Woo, pp111-134. New York: Kluwer/Plenum.

139. Schubert V, Schubert PA, Breit G, Intaglietta M. 1995. Analysis of arterial flowmotion in spinal-cord injured and elderly subjects in an area at risk for the development of pressure ulcers. *Paraplegia* 33:387-397.

140. Li ZY, Tam EWC, LEUNG JYS, Mak AFT. 2006. Wavelet Analysis of Skin Blood Oscillations in Persons with Spinal Cord Injury and Normal Subjects. *Arch. Phys. Med. Rehabil.* 87:1207-1212.

141. Bollinger A, Hoffman U, Franzeck UK. 1991. Evaluation of flowmotion in man by laser Doppler technique. *Blood Vessels* 28(Suppl.1):21–26.

142. Bracic M, Stefanovska A. 1998. Wavelet based analysis of human blood flow dynamics. *Bull. Math. Biol*. 60:919–935.

143. Kvernmo HD, Stefanovska A, Kirkeboen KA. 2003. Enhanced endothelial activity reflected in cutaneous blood low oscillations of athletes. *Eur. J. Appl. Physiol.*90:16-22

144. Bertuglia S, Colantuoni A, Arnold M, Witte H. 1996. Dynamic coherence analysis of vasomotion and flow motion in skeletal muscle microcirculation. *Microvascular Research*. 52:235-244

145. Stefanovska A, Bracic M, Kvernmo HD. 1999. Wavelet analysis of oscillations in the peripheral blood circulation measured by laser Doppler technique. *IEEE Trans. Biomed. Eng.* 46:1230–1239.

146. Soderstrom T, Stefanovska A, Veber M, Svensson H. 2003 Involvement of sympathetic nerve activity in skin blood flow oscillations in humans. *Am J Physiol Heart Circ Physiol.* 284:H1638–H1646.

147. Bergstrand S, Lindberg LG, Ek AC, Linden M, Lindgren M. 2009. Blood flow measurements at different depths using photoplethysmography and laser Doppler techniques. *Skin Res. & Tech.* 15:139-147.

148. Sanders JE, Goldstein BS. 2001. Collagen fibril diameters increase and fibril densities decrease in skin subjected to repetitive compressive and shear stresses. *J. Biomech.* 34:1581-1587.

149. Sanders JE, Mitchell SB, Wang YN, Wu K. 2002. An explants model for the investigation of skin adaptation to mechanical stress. *IEEE Trans. Biomed. Eng*. 49:1626-1631.

150. Saito Y, Hasegawa M, Fujimoto M, Matsushita T, Horikawa M, Takenaka M, Ogawa F, Sugama J, Steeber DA, Sato S, Takehara K. 2008. The loss of MCP-1 attenuates cutaneous ischemia-reperfusion injury in a mouse model of pressure ulcer. *J Invest. Dermatology* 128: 1838-1851.

151. Blaisdell FW. 2002. The pathophysiology of skeletal muscle ischemia and the reperfusion syndrome: a review. *Cardiovascular Surgery* 10:620-630.

152. Unal S, Ozmen S, Demir Y, Yavuzer R, Latifoglu O, Atabay K. 2001. The effect of gradually increased blood flow on ischemia-reperfusion injury. *Ann. Plast. Surg*. 47: 412-416.

153. Nola GT, Vistnes LM. 1980. Differential response of skin and muscle in the experimental production of pressure sore. *Plast. & Reconst. Surg*. 66:728-733.

154. Stekelenburg A, Oomens CWJ, Strijkers GJ, Nicolay K, Bader DL. 2006. Compression-induced deep tissue injury examined with magnetic resonance imaging and histology. *J. Appl. Physiol.* 100:1946-1954.

155. Kwan MPC, Tam EWC, Lo SCL, Leung MCP, Lau RYC. 2007. The time effect of pressure on tissue viability: investigation using an experimental rat model. *Exp. Biol. Med.* 232:481-487.

156. Linder-Ganz E, Gefen A. 2004. Mechanical compression-induced pressure sores in a rat hindlimb: muscle stiffness, histology, and computational models. *J. Appl. Physiol*. 96:2034-2049.

157. Linder-Ganz E, Engelberg S, Scheinowitz M, Gefen A. 2006. Pressure-time cell death threshold for albino rat skeletal muscles as related to pressure sore biomechanics. *J. Biomech.* 39:2725-2732.

158. Peeters EAG, Oomens CWJ, Bouten CVC, Bader DL, Baaijens FPT. 2005. Mechanical and failure properties of single attached cells under compression. *J. Biomech.* 38:1685-1693.

159. Bouten CVC, Knight MM, Lee DA, Bader DL. 2001. Compressive deformation and damage of muscle cell subpopulations in a model system. *Ann. Biomed. Eng*. 29:153-163.

160. Breuls RGM, Bouten CVC, Oomens CWJ, Bader DL, Baaijens FPT. 2003. Compression induced cell damage in engineered muscle tissue: an in vitro model to study pressure ulcer aetiology. *Ann. Biomed. Eng.* 31:1357-1364.

161. Gawlitta D, Li w, Oomens CWJ, Baaijens FPT, Bader DL, Bouten CVC. 2006. The relative contributions of compression and hypoxia to development of muscle tissue damage: an in vitro study. *Ann Biomed. Eng*. 35:273-284.

162. Gefen A, Nierop BV, Bader DL, Oomens. 2008. Strain-time cell-death threshold dor skeletal nmuscle in a tissue-engineered model system for deep tissue injury. *J. Biomech*. 41:2003-2012.

163. Ceelen KK, Ooemns CWJ, Stekelenburg A, Bader DL, Baaijens FPT. 2009. Changes in intracellular calcium during compression of C2C12 myotubes. *Exp. Mech*. 49:25-33.

164. Siu PM, Tam EW, Teng BT, Pei XM, Ng JW, Benzie IF, Mak AF. 2009. Muscle apoptosis is induced in pressure-induced deep tissue injury. *J. Appl. Physiol*. Paper accepted.

165. Linder-Ganz E, Gefen A. 2009. Stress analysis coupled with damage laws to determine biomechanical risk factors for deep tissue injury during sitting. *ASME J. Biomech. Eng.* 131: 011003-1 – 011003-13.

166. Ceelen KK, Oomens CWJ, Baaijens FPT. 2008. Microstructural analsysis of deformation-induced hypoxic damage in skeletal muscle. *Biomech. Model Mechanobiol*. 7:277-284.

Figure 1

Positions of ischial tuberosities and their corresponding peak pressures on pressure map during dynamic wheelchair propulsion (one normal subject). The peak pressure locations are anterior to the locations of the ischial tuberosities.

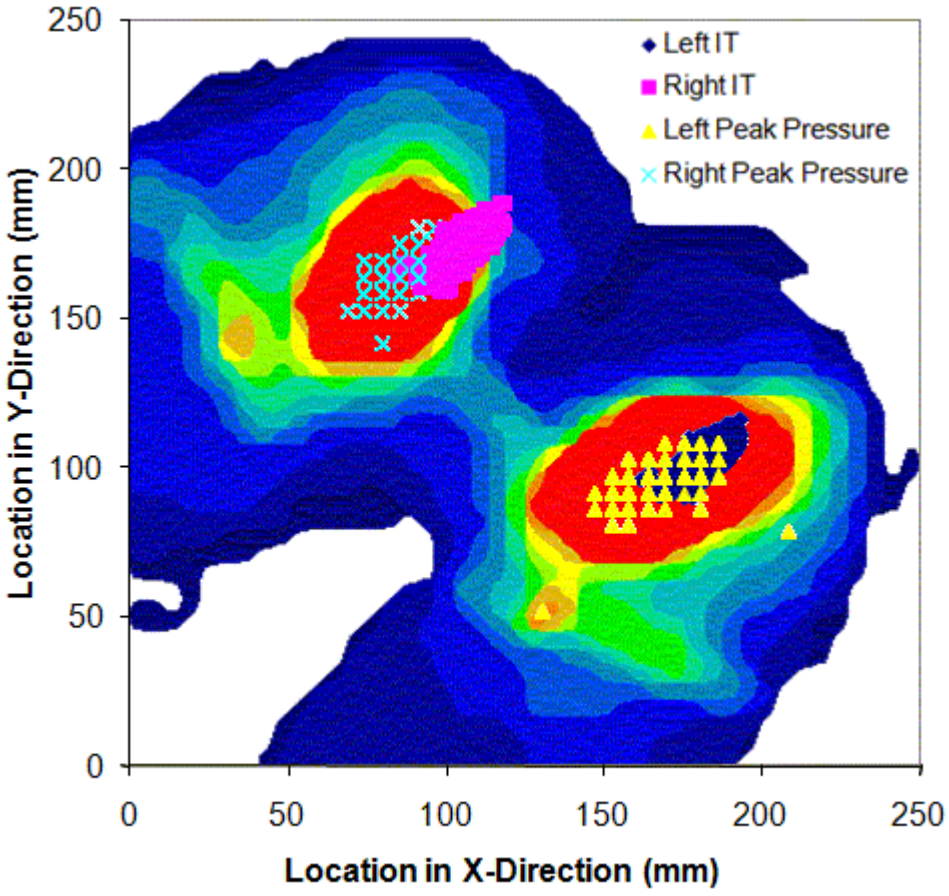

Figure 2

Schematic representation of a reactive hyperaemic response.

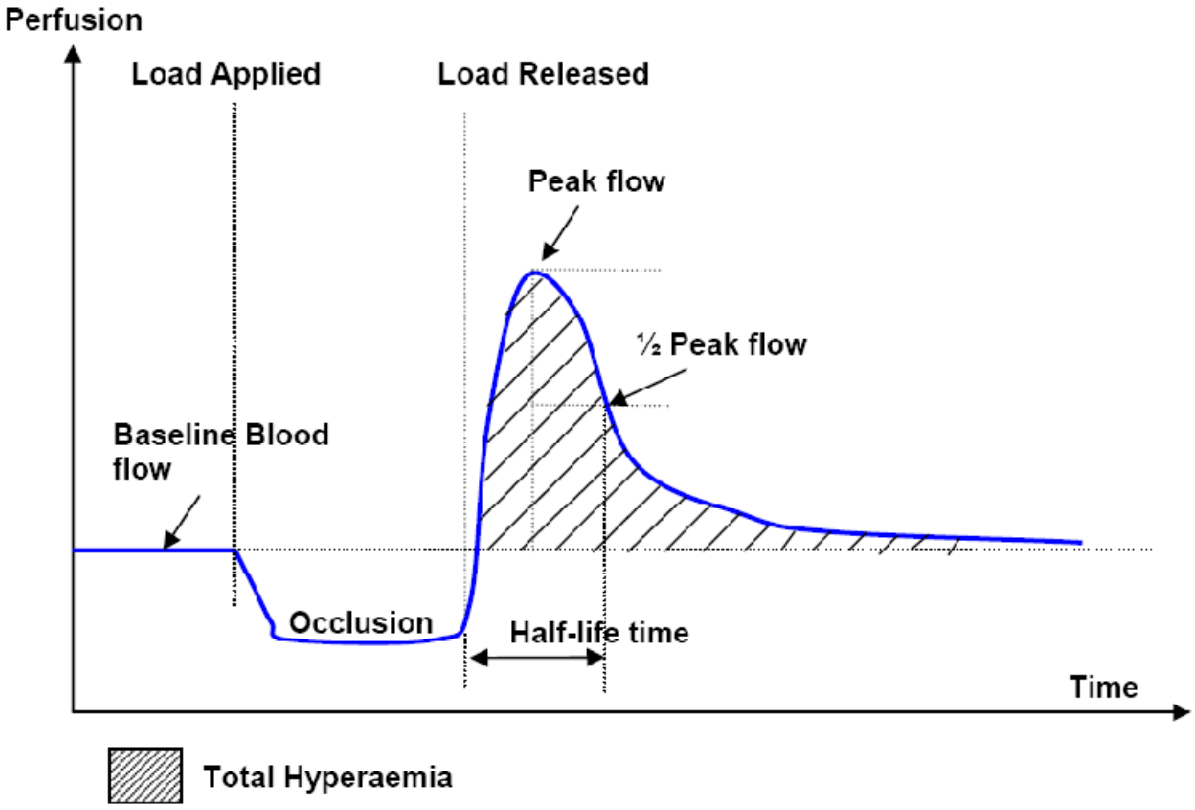

Figure 3
Photomicrograph of muscle fibres at the tibialis area. (155) (A) Normal muscle architecture of control rat shows closely packed polygonal muscle fibre profiles. There is little variation in muscle fibre size or shape. Cytoplasmic staining is uniform. Small, peripherally located nuclei are abundant. (B) Muscle fibres at 48hr, degeneration of muscle cells is characterized by increasingly numerous nuclei, which occupy the central part of the muscle fibres. (C) At 72hr, atrophic and hypertrophic muscle fibres with round contours are present. (D) At 96hr, muscle fibres are replaced by fibro-fatty tissue, with abnormal variation in fibre size due to atrophy of some and hypertrophy of others. (E) At 96hr, muscle fibres become necrotic. Peripherally located nuclei of muscle fibres become internalized. There is destruction of muscle fibres with replacement of the muscle by fibrous tissue. (F) At 168hr, muscle fibres become severely necrotic, where muscle atrophy affects groups of muscle fibres supplied by single motor units in contrast to the haphazard pattern of atrophy seen at other groups. (H&E, x30)